



# Astragaloside IV enhances the sensitivity of breast cancer stem cells to paclitaxel by inhibiting stemness

Ping Huang<sup>1,2#</sup>, Huachao Li<sup>2#</sup>, Liping Ren<sup>2#</sup>, Haimei Xie<sup>2</sup>, Liushan Chen<sup>2,3</sup>, Yuqi Liang<sup>2</sup>, Yuyu Hu<sup>2,3</sup>, Heloisa Sobreiro Selistre-de-Araujo<sup>4</sup>, Stergios Boussios<sup>5,6,7,8</sup>, Sachin R. Jhavar<sup>9</sup>, Rutao Cui<sup>10</sup>, Qian Zuo<sup>2</sup>, Qianjun Chen<sup>1,2,3</sup>

<sup>1</sup>State Key Laboratory of Traditional Chinese Medicine Syndrome, The Second Affiliated Hospital of Guangzhou University of Chinese Medicine, Guangzhou, China; <sup>2</sup>Department of Breast, Guangdong Provincial Hospital of Chinese Medicine, Guangzhou, China; <sup>3</sup>Guangdong Academy of Chinese Medicine, Guangzhou, China; <sup>4</sup>Biochemistry and Molecular Biology Laboratory, Department of Physiological Sciences, Universidade Federal de São Carlos (UFSCar), São Carlos, Brazil; <sup>5</sup>Department of Medical Oncology, Medway NHS Foundation Trust, Kent, UK; <sup>6</sup>Faculty of Life Sciences & Medicine, School of Cancer & Pharmaceutical Sciences, King's College London, London, UK; <sup>7</sup>Kent Medway Medical School, University of Kent, Kent, UK; <sup>8</sup>AELIA Organization, Thessaloniki, Greece; <sup>9</sup>Department of Radiation Oncology, The Ohio State University Wexner Medical Center, Columbus, OH, USA; <sup>10</sup>Zhejiang University School of Medicine, Hangzhou, China

**Contributions:** (I) Conception and design: Q Chen; (II) Administrative support: Q Zuo; (III) Provision of study materials or patients: Q Chen, R Cui; (IV) Collection and assembly of data: P Huang, H Li; (V) Data analysis and interpretation: P Huang, L Ren; (VI) Manuscript writing: All authors; (VII) Final approval of manuscript: All authors.

<sup>#</sup>These authors contributed equally to this work.

**Correspondence to:** Qianjun Chen, MD. State Key Laboratory of Traditional Chinese Medicine Syndrome, The Second Affiliated Hospital of Guangzhou University of Chinese Medicine, 55 N, Neihuanxi Road, Guangzhou 510006, China; Department of Breast, Guangdong Provincial Hospital of Chinese Medicine, 111 N, Dade Road, Guangzhou 510120, China; Guangdong Academy of Chinese Medicine, 55 N, Neihuanxi Road, Guangzhou 510006, China. Email: cqj55@163.com; Qian Zuo, MD. Department of Breast, Guangdong Provincial Hospital of Chinese Medicine, 111 N, Dade Road, Guangzhou 510120, China. Email: 827649822@qq.com; Rutao Cui, MD. Zhejiang University School of Medicine, 866 Yuhangtang Road, Hangzhou 310058, China. Email: rutaocui@hotmail.com.

**Background:** Chemotherapy is one of the common treatments for breast cancer. The induction of cancer stem cells (CSCs) is an important reason for chemotherapy failure and breast cancer recurrence. Astragaloside IV (ASIV) is one of the effective components of the traditional Chinese medicine (TCM) *Astragalus membranaceus*, which can improve the sensitivity of various tumors to chemotherapy drugs. Here, we explored the sensitization effect of ASIV to chemotherapy drug paclitaxel (PTX) in breast cancer from the perspective of CSCs.

**Methods:** The study included both *in vitro* and *in vivo* experiments. CSCs from the breast cancer cell line MCF7 with stem cell characteristics were successfully induced *in vitro*. Cell viability and proliferation were detected using the Cell Counting Kit-8 (CCK-8) and colony formation assays, and flow cytometry and terminal deoxynucleotidyl transferase dUTP nick end labeling (TUNEL) methods were performed to detect cell apoptosis. Stemness-related protein expression was determined by western blotting (WB) and immunohistochemistry (IHC). Body weight, histopathology, and visceral organ damage of mice were used to monitor drug toxicity.

**Results:** The expression of stemness markers including Sox2, Nanog, and ALDH1 was stronger in MCF7-CSCs than in MCF7. PTX treatment inhibited the proliferation of tumor cells by promoting cell apoptosis, whereas the stemness of breast cancer stem cells (BCSCs) resisted the effects of PTX. ASIV decreased the stemness of BCSCs, increased the sensitivity of BCSCs to PTX, and synergistically promoted PTX-induced apoptosis of breast cancer cells. Our results showed that the total cell apoptosis rate increased by about 25% after adding ASIV compared with BCSCs treated with PTX alone. The *in vivo* experiments demonstrated that ASIV enhanced the ability of PTX to inhibit the growth of breast cancer. WB and IHC showed that ASIV reduced the stemness of CSCs.

**Conclusions:** In this study, the resistance of breast cancer to PTX was attributed to the existence of CSCs;

ASIV weakened the resistance of MCF7-CSCs to PTX by significantly attenuating the hallmarks of breast cancer stemness and improved the efficacy of PTX.

**Keywords:** Breast cancer; cancer stem cells (CSCs); astragaloside IV (ASIV); paclitaxel (PTX); chemotherapy

Submitted Oct 12, 2023. Accepted for publication Nov 22, 2023. Published online Dec 21, 2023.

doi: 10.21037/tcr-23-1885

View this article at: <https://dx.doi.org/10.21037/tcr-23-1885>

## Introduction

The incidence of breast cancer in women (11.7%) has surpassed that of lung cancer (11.4%) to become the most common malignancy worldwide (1). While the majority of breast cancer cases are detected at an early stage, with a corresponding 5-year survival rate of 96% in Europe, advanced breast cancer remains an incurable condition (2). Breast cancer is a remarkably diverse disease, displaying a wide range of clinical behaviors and molecular drivers. This diversity necessitates a complex array of therapeutic approaches grounded in a deep understanding of its biological foundations (3). Breast cancer can be categorized based on the expression of hormone receptors, specifically estrogen and progesterone receptors, as well as the presence of human epidermal growth factor receptor 2 (HER2) overexpression and/or gene amplification. These factors are evaluated through techniques like immunohistochemistry

(IHC) and *in situ* hybridization (4,5). This biological characterization is paramount not only for determining the prognosis of breast cancer patients but also for guiding treatment decisions (6).

There are currently multiple treatments for breast cancer, including surgery, radiotherapy (RT), chemotherapy, endocrine therapy, and targeted therapy. While the inception of cancer immunotherapy for breast cancer dates back over two decades, its adoption in patient care lagged behind that in other cancer types. However, the ongoing and robust clinical research endeavors hold promise in altering this scenario, paving the way for the broader application of immune checkpoint inhibitors and various immunotherapies in breast cancer, extending their reach beyond just the triple-negative breast cancer (TNBC) subtype (7). Although improvements and developments in diagnostic methods, surgical techniques, and pre- and postoperative treatment have increased the survival rate of breast cancer, tumor recurrence and metastasis still occur in 30–40% of patients (8).

Chemotherapy is an important treatment for early and advanced breast cancer (9); however, cancer stem cells (CSCs) are an important cause of chemotherapy failure and breast cancer recurrence (10,11). CSCs are a subset of cells found in tumor tissues with the hallmarks of breast cancer stemness, which are the drivers of cancer progression and are closely related to tumor metastasis, recurrence, and drug resistance (12). Studies have shown that breast cancer stem cells (BCSCs) are resistant to standard chemotherapeutic drugs, and BCSCs that survive treatment can re-enter the cell proliferation cycle and form new tumor lesions in a specific environment, leading to breast cancer recurrence and metastasis (10,13). Therefore, targeting CSCs may be a promising therapeutic strategy to effectively improve chemotherapy sensitivity and consequentially increase cure rates.

Paclitaxel (PTX) is an anti-microtubule chemotherapeutic agent that has been successfully used in different types of

### Highlight box

#### Key findings

- Astragaloside IV (ASIV) attenuated the stemness of cancer stem cells (CSCs).
- The ability of ASIV to reduce the stemness of CSCs is the main reason for increasing the sensitivity of breast cancer stem cells to paclitaxel (PTX).

#### What is known and what is new?

- Chemotherapy is often employed in the treatment of breast cancer. The induction of CSCs is an important reason for chemotherapy failure and breast cancer recurrence.
- ASIV weakened the resistance of MCF7-CSCs to PTX by significantly attenuating the hallmarks of breast cancer stemness and improved the efficacy of PTX in breast cancer.

#### What is the implication, and what should change now?

- Our study provides an experimental basis for the synergistic effect of ASIV with breast cancer chemotherapy.
- The current our work does not explain how ASIV affects the stemness of tumor cells, so we will further explore the mechanism.

solid tumors, including breast cancer (14-17). Presently, PTX is a first-line chemotherapy drug for breast cancer, although it is prone to drug resistance during the treatment process (18). A growing number of studies have focused on improving tumor sensitivity to PTX, including combination therapy using natural compounds with PTX (19-22).

The traditional Chinese herb *Astragalus mongholicus* Bunge (AM; Huang qi in Chinese pin yin) is widely used by traditional Chinese medicine (TCM) practitioners. Modern pharmacological studies have shown that AM and its active components have various pharmacological effects such as the prevention and treatment of viruses, tumors, and diabetes, as well as the regulation of cardiovascular and immunity (23,24). Astragaloside IV (ASIV) is one of the active ingredients of AM. ASIV has a wide range of pharmacological effects, such as antioxidant, cardioprotective, anti-inflammatory, antiviral, antibacterial, antifibrotic, antidiabetic, antitumor, and immunomodulatory effects. It has a protective effect on brain damage and the central nervous system, cardiovascular disease, respiratory system, kidney, endocrine system, organic immune system, and liver (25-27). Moreover, ASIV plays an anti-cancer role in tumors such as lung, liver, colorectal, and breast cancer (28-36). Studies have found that ASIV improved the sensitivity of various cancers to chemotherapy, as follows: ASIV improved the sensitivity of osteosarcoma cells to cisplatin via apoptosis induction and regulation of caspase-dependent Fas/FasL signaling (28); ASIV enhanced the sensitivity of lung adenocarcinoma cells to bevacizumab by inhibiting autophagy (30); ASIV enhanced the sensitivity of breast cancer to PTX by targeting caveolin-1-mediated oxidative damage (37).

Although researchers have explored the synergistic effect of ASIV on chemotherapeutic drugs from various aspects, the effect of ASIV on chemoresistance in CSCs is still unknown. Here, we aimed to investigate the effect of ASIV combined with PTX, a breast cancer chemotherapy drug, on CSCs and its underlying mechanism. We present this article in accordance with the ARRIVE and MDAR reporting checklists (available at <https://tcr.amegroups.com/article/view/10.21037/tcr-23-1885/rc>).

## Methods

### *Cell culture and reagents*

The human luminal breast cancer cell line MCF-7 was purchased from Procell (Wuhan, China), cultured in Dulbecco's

modified Eagle medium (DMEM) with 10% fetal bovine serum (FBS), and incubated in the incubator with a constant temperature incubator of 37 °C and 5% CO<sub>2</sub>. ASIV [No. 84687-43-4, purity: high-performance liquid chromatography (HPLC) ≥98%, molecular formula: C<sub>41</sub>H<sub>68</sub>O<sub>14</sub>, molecular weight: 784.97, density: 1.39 g/cm<sup>3</sup>] was purchased from Chengdu Ruifensi Biological Technology Co., Ltd. (Chengdu, China). PTX was purchased from Hainan All Star Pharmaceutical Co., Ltd. (Haikou, China).

### *Induction of MCF7-CSCs*

MCF7-CSCs came from the human breast cancer cell line MCF7 that was induced as previously described (38). Serum-free medium (SFM) consisted of DMEM/F12, 20 ng/mL basic fibroblast growth factor (Proteintech, Wuhan, China), 10 ng/mL epidermal growth factor (Proteintech), and 1×B27 supplement (Gibco Life Technologies, Lofer, Austria). When MCF7 cell density reached 90%, the cell precipitate was rinsed with phosphate-buffered saline (PBS), centrifuged at 1,000 rpm for 5 minutes, and the supernatant was discarded. MCF7 cells were resuspended in SFM, and the cell suspension was transferred to non-adherent culture flasks.

### *Cell viability analysis*

Before treatment, the cell (including MCF7 and MCF7-CSCs) concentration was adjusted to 3,000 cells/100 µL, and they were seeded in 96-well plates with 100 µL per well and cultured for 24 hours. Cells were then treated with ASIV and PTX alone or in combination for 48 hours. After 48 hours, 10 µL of Cell Counting Kit-8 (CCK-8; Beyotime, Jiangsu, China, C0039) solution was added per well and incubated at 37 °C for 2 hours. Plate Reader was used to determine the optical density (OD) value at 450 nm. Biological replicates were repeated 3 times. The half maximal inhibitory concentration (IC<sub>50</sub>) was calculated with Prism 7 (GraphPad software, San Diego, CA, USA).

### *Stem cell detection by flow cytometry*

To assess whether the breast cancer-related stem cell clones (CD44<sup>+</sup>/CD24<sup>-</sup>/low) were successfully induced, cells underwent fluorescein isothiocyanate (FITC)-labeled anti-CD24 antibody (Biolegend, San Diego, CA, USA; 311104) and allophycocyanin (APC)/Cy7-labeled anti-CD44 antibody [Becton, Dickinson and Company (BD), Franklin

Lakes, NJ, USA; 559942] staining and flowcytometry assessment. Subsequently, cells were washed with cold PBS containing 10% fetal calf serum (FCS). After staining with anti-CD44 and anti-CD24 antibodies, incubate for 30 minutes at room temperature protected from light. After three washes with cold PBS containing 10% FCS, cells were collected. The fluorescence signals of FITC and APC/Cy7 were analyzed, respectively.

### **Western blot (WB)**

The experimental group was defined using a predetermined experimental drug concentration (single or combination), while the drug-free medium was defined as a control group, with each group acting on the cells for 48 hours. After treatment, cells were collected for lysis. Protein concentration was determined using the bicinchoninic acid (BCA) Protein Assay Kit (Keygen, Nanjing, China). Samples of 20 µg of protein were collected, resolved in a 10% sodium dodecyl sulfate polyacrylamide gel electrophoresis (SDS-PAGE), and transferred to a polyvinylidene fluoride (PVDF) membrane. Then, 5% blocking buffer [5% skimmed milk powder + tris-buffered saline with Tween 20 (TBST)] was applied to the membrane for 60 minutes at room temperature. Subsequently, the membrane was incubated with primary antibodies, including Sox2 antibody (Proteintech, 11064-1-AP), Oct4 antibody (Abcam, Cambridge, UK; ab200834), beta-actin (Proteintech, 66009-1-Ig), Bcl2 antibody (Abcam, mab182858), Bax antibody (Proteintech, 50599-2-Ig), glyceraldehyde-3-phosphate dehydrogenase (GAPDH) antibody (Proteintech, 10494-1-AP), Nanog antibody [Cell Signaling Technology (CST), Danvers, MA, USA; 4903T] overnight at 4 °C. The next day, secondary antibodies were added and the membranes were washed and visualized using ChemiDoc TMXRS+ (Bio-Rad, Hercules, CA, USA) after 60 minutes of incubation at room temperature.

### **Cell apoptosis analysis**

The apoptosis of cells was analyzed by annexin-v-FITC/propidium iodide (PI) staining flow cytometry. Cells with an initial cell number of  $2 \times 10^6$  cells/mL were seeded on 6-well plates and exposed to different doses of ASIV and PTX alone or in combination for 48 hours. Staining was accorded to the manufacturer's instructions (Keygen). Samples were analyzed using flow cytometry FC500 (Beckman Coulter, Inc., Brea, CA, USA). FITC-annexin V-positive and PI-

negative cells are considered to be a subset of cells with early apoptosis. Cells that are positive for FITC-annexin V and PI were calculated to be a subset of cells with late apoptosis. Experiments were conducted in triplicate.

### **Experimental animals, drug dosages**

We purchased 5-week-old Balb/c-nu/nu female mice from the Animal Experiment Center of Guangdong Provincial Hospital of Chinese Medicine. All mice were housed in cages (3–5 mice per cage) under pathogen-free conditions at 25 °C, 40–60% relative humidity, and 12 hours light/dark cycle in the experimental animal center of Guangdong Provincial Hospital of Chinese Medicine. Animal experiments were performed under a project license (No. 2022008) granted by The Institutional Animal Research Ethics Committee of Guangdong Provincial Hospital of Chinese Medicine, in compliance with national guidelines for the care and use of animals. A protocol was prepared before the study without registration.

We consulted a large body of literature when choosing doses. For the *in vivo* studies of resistance to PTX by MCF7 and MCF7-BCSC, we first selected the drug concentration provided in the previous literature at a concentration of 5 mg/kg, comprising intraperitoneal injection once every other day for a total of 21 days (39). Differences were observed in both groups of mice, so this dose was continued in combination with PTX and ASIV, and in most of the literature, ASIV was used directly with a single dose for animal experiments, with dose ranges ranging from 20 to 100 mg/kg. Therefore, we first selected 40 mg/kg for preliminary experiments and obtained positive results in subsequent experiments.

ASIV was suspended in a solution consisting of 5% dimethyl sulfoxide (DMSO), 40% polyethylene glycol 300 (PEG300), and 45% saline, and administered once daily via gastric perfusion. PTX was diluted with saline and administered via intraperitoneal injection every other day. The control group received the vehicle (5% DMSO + 40% PEG300 + 45% saline) via intragastric perfusion and saline via intraperitoneal injection.

### **Breast cancer xenografts in nude mice**

We conducted three different animal experiments. Animals were included if the *in vivo* transplanted tumor model was successfully constructed, and animals that died prematurely were excluded. Animal experiments were conducted by two

people, one for execution and one for testing, to ensure the reliability of the data.

First, mice were randomly divided into experimental and control groups (n=7 in each group), and then MCF7 and MCF7-CSCs cells were injected into the mammary fat pads of the control group and the experimental group, respectively. The cell density of each group was  $5 \times 10^6$  cells/200  $\mu$ L PBS. After 21 days, the mice were euthanized and the tumor growth of the two groups was compared.

In another animal experiment, mice were randomly divided into experimental and control groups (n=7 in each group), and then MCF7 and MCF7-CSCs cells were injected into the mammary fat pads of the control group and the experimental group. Upon reaching a tumor volume of approximately 100 mm<sup>3</sup>, PTX (5 mg/kg) was used on each group of mice. The length and width of tumors in each mouse were recorded using vernier calipers every 2–3 days, tumor volume was calculated using the formula  $[0.5 \times (\text{length}) \times (\text{width})^2]$ . After 21 days, the mice were euthanized and the tumor growth of the two groups was compared.

A similar experiment was conducted, wherein  $5 \times 10^6$  MCF7-CSCs were injected into the mammary fat pads of mice in 200  $\mu$ L PBS. Upon reaching a tumor volume of approximately 100 mm<sup>3</sup>, the mice were randomly divided into control and treatment groups (n=6) as follows: control group; ASIV group (40 mg/kg); PTX group (5 mg/kg); and PTX (40 mg/kg) combined with ASIV (5 mg/kg) group. Different groups of mice were treated with the appropriate drug. The length and width of tumors in each mouse were recorded using vernier calipers every 2–3 days, tumor volume was calculated using the formula  $[0.5 \times (\text{length}) \times (\text{width})^2]$ . After 21 days, the mice were euthanized and the tumor growth of the two groups was compared. Throughout the entire experiment, we meticulously monitored the subjects' body weight to ascertain any potential toxicity of the administered drugs.

### IHC

For tissue embedding, specimens were fixed in 10% neutral buffered formalin for 24 hours. After being cut into 3  $\mu$ m-thick sections, the paraffin-embedded tumor samples were dried overnight at 37 °C. The sections underwent two rounds of xylene deparaffinization, each lasting 10 minutes, followed by rehydration via a graded series of ethanol. The sections were incubated at an ambient temperature in a 3% hydrogen peroxide solution for a duration of 30 minutes

to effectively hinder the activity of endogenous peroxidase. We heated the slides in a sodium-citrate buffer solution to retrieve the antigen. The slides were then incubated with the primary antibodies including anti-SRY-box 2 (Sox2; Proteintech, 11064-1-AP), and anti-Nanog (CST, 4903T) at 4 °C overnight in a moist chamber. A diaminobenzidine detection system was applied as the chromogenic agent according to the manufacturer's instructions. As a final step, the sections were counterstained with Mayer's hematoxylin, dehydrated, cleared, and mounted before the examinations.

### 3-dimensional (3D) sphere assay

This experiment was conducted as previously described (40). T7 buffer (pH 7.4, containing 50 mM Tris and 150 mM NaCl) was employed to dilute fibrinogen to a concentration of 2 mg/mL. In 2-dimensional (2D) rigid culture dishes, MCF7 cells were gently detached and adjusted to a concentration of  $10^4$  cells/mL. The fibrinogen solution and cell solution were combined in equal proportions, resulting in a meticulously crafted mixture of fibrin gels containing 1 mg of fibrinogen per mL and a concentration of 5,000 cells/mL. The 96-well plates were seeded with a mixture of 50  $\mu$ L of cells and fibrinogen, to which 1  $\mu$ L of thrombin (100 U/mL) was added and mixed well. The cell culture plate was then placed in an incubator at 37 °C for 10 minutes. Finally, 200  $\mu$ L of DMEM medium supplemented with 10% FBS and antibiotics were introduced.

### Statistical analysis

The data acquired were expressed as mean (standard deviation), median (range), or frequency (percentage). The independent samples *t*-test (for normally distributed data) or the Mann-Whitney *U* test (for non-normally distributed data) were employed to compare any two groups.

## Results

### Induction of MCF7-CSCs

To investigate the sensitization effect of ASIV on CSCs, we successfully induced MCF7-CSC following a previously published method (38). CD44(high)/CD24(low) cell populations were identified as BCSCs; this subpopulation of cells was significantly increased in MCF7-CSCs after induction, and the expression of CSCs marker aldehyde dehydrogenase 1 family member A1 (ALDH1) was

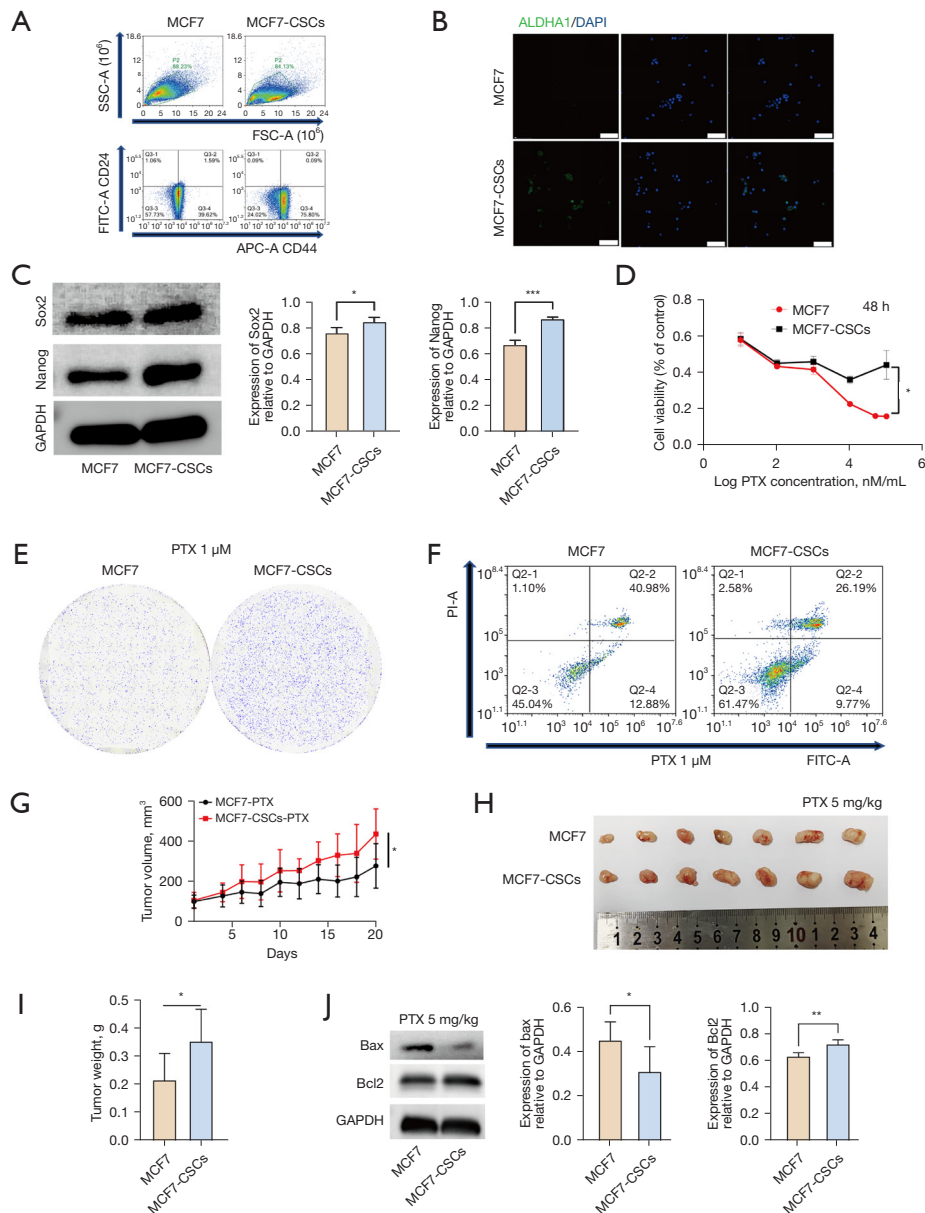


**Figure 1** Induction and identification of MCF7-CSCs, detection of resistance of MCF7-CSCs to PTX. (A) Changes in tumor stem cells [CD44(high)/CD24(low)] before and after induction were detected by flow cytometry. (B) Immunofluorescence was used to detect the expression of stem cell marker ALDH1 in MCF7 and MCF7-CSCs (scale bar: 100 μm). (C) Western blotting was used to detect the expression of stem cell markers Sox2 and Nanog proteins in MCF7 and MCF7-CSCs. (D) MCF7 and MCF7-CSCs were treated with different concentrations of PTX for 48 h, and cell viability was detected using the CCK-8. (E) 10,000 MCF7 and MCF7-CSCs cells homogeneously seeded in 6-well plates, cells were treated with 1 μM PTX for 48 h, PTX was removed, and cell culture continued for 12 d. Formaldehyde fixed, crystal violet stained. The effect of PTX on the proliferation of the two cells was detected by colony formation assay. (F) After the two kinds of cells were treated with PTX for 48 h, apoptosis was detected by cell flow cytometry. The effect of PTX on the growth of MCF7 and MCF7-CSCs in nude mice was detected: the tumor growth curve (G), tumor image (H), and tumor weight (I) were detected. (J) Western blotting was used to detect apoptosis-related protein Bax/Bcl2 expression in animal tumor tissues. Student's *t*-test: \*,  $P < 0.05$ ; \*\*,  $P < 0.01$ ; \*\*\*,  $P < 0.001$ . SSC, side scatter; CSCs, cancer stem cells; FSC, forward scatter; FITC, fluorescein isothiocyanate; APC, allophycocyanin; ALDH1, aldehyde dehydrogenase 1 family member A1; DAPI, 4',6-diamidino-2-phenylindole; PTX, paclitaxel; PI, propidium iodide; CCK-8, Cell Counting Kit-8.

increased in MCF7-CSCs (Figure 1A,1B). The results of WB showed that the levels of stemness-related markers Sox2 and Nanog were significantly increased in MCF7-CSCs (Figure 1C). The above results represent the successful induction of MCF7-CSCs.

### ***Tumor cell stemness is crucial for the anticancer effect of PTX***

We examined the inhibitory effects of PTX on the proliferation of MCF7 and MCF7-CSCs cells at different time points. The results showed no difference between MCF7 and MCF7-CSCs with PTX treatment for 24 hours (Figure S1); however, with 48 hours PTX treatment, MCF7 cells showed higher inhibition of proliferation than the MCF7-CSCs (Figure 1D). Since 1  $\mu$ M PTX elicited a significant difference in the inhibition of the proliferation of the two types of cells, PTX was used at 1  $\mu$ M for subsequent experiments. The clonogenic assay also demonstrated that PTX inhibited the proliferation of MCF7-CSCs (Figure 1E). Apoptosis experiments showed that PTX could inhibit cell proliferation by inducing apoptosis, and MCF7-CSCs were resistant to the apoptotic effect of PTX on cells (Figure 1F). In addition, we further evaluated the resistance of MCF7 and MCF7-CSCs to PTX by *in vivo* experiments in mice. After the same amount of MCF7 and MCF7-CSCs were injected into mice, no difference in tumor size or tumor weight was observed 21 days later (Figure S2). Consistent with the results from *in vitro* experiments, the increased stemness of breast cancer cells resisted the inhibitory effect of PTX on tumor growth (Figure 1G). The tumor volume and body weight of the mice in the MCF7-CSC group were significantly higher than those of the MCF7 group (Figure 1H,1I). The WB analysis of tumor tissues showed that the cell's stemness can increase the expression of anti-apoptotic protein Bcl2 and decrease the expression of apoptosis marker Bax under the effect of PTX (Figure 1f). The above results indicate that PTX can inhibit the proliferation of tumor cells by promoting cell apoptosis, whereas the increased stemness of tumor cells can resist the effect of PTX.

### ***ASIV synergizes with PTX to inhibit BCSC proliferation***

Next, we verified the chemosensitizing effect of ASIV. The chemical structure of ASIV is shown in Figure 2A. The CCK-8 and clone formation assays showed that ASIV alone did not inhibit the proliferation of MCF7-

CSCs at the tested concentrations, but when combined with PTX, it significantly inhibited the proliferation of MCF7-CSCs. However, the inhibitory effect of PTX on cell proliferation was significantly increased when ASIV was increased (Figure 2B,2C). Moreover, the results of cytometry showed that ASIV increased PTX-induced apoptosis, compared with control MCF7-CSCs cells ( $2.6\% \pm 0.2\%$ ), PTX alone induced significant apoptosis ( $15.8\% \pm 0.6\%$ ) after 48 h of exposure, while ASIV alone did not increase apoptosis ( $1.4\% \pm 0.1\%$ ). However, compared with PTX alone, PTX combined with ASIV induced more apoptosis ( $20.7\% \pm 1.1\%$ ). Among them, the early apoptosis rates of MCF7-CSCs cells induced by ASIV, PTX and their combination were  $0.9\% \pm 0.1\%$ ,  $10.1\% \pm 0.9\%$  and  $13.7\% \pm 0.8\%$ , respectively ( $1.7\% \pm 0.1\%$  in the control group) (Figure 2D).

### ***ASIV enhances the ability of PTX to inhibit breast cancer growth***

To determine the role of ASIV in breast cancer chemotherapy, we conducted animal experiments (Figure 3A), the same number of MCF7-CSCs were injected into the mammary fat pad of mice, and the growth of subcutaneous tumors in mice was observed under different treatment conditions the use of different drug groups. In this experiment, we found that MCF7-CSCs showed resistance to PTX; PTX treatment did not slow down the growth of breast cancer. Addition of ASIV to PTX, however, significantly inhibited the growth of breast cancer (Figure 3B). We found that tumor weight was also affected by PTX plus ASIV (Figure 3C) and tumors of different groups of mice were photographed (Figure 3D). WB and terminal deoxynucleotidyl transferase dUTP nick end labeling (TUNEL) staining results of tumor tissues also showed that the combination of ASIV and PTX increased the level of apoptosis in breast cancer cells (Figure 3E,3F). Next, we evaluated the toxic effects of the drugs; ASIV and PTX did not affect the body weight of the mice (Figure S3A), and hematoxylin and eosin (H&E) staining results showed that treatment with the combination of the two did not increase the damage to important organs (Figure S3B).

### ***ASIV combined with PTX reduces the stemness of BCSC***

Sphere-forming ability is an important method for the identification of CSCs *in vitro*. Here, we evaluated the cell stemness by examining the size of the tumor sphere. First, we observed the formation of MCF7 and MCF7-CSCs stem

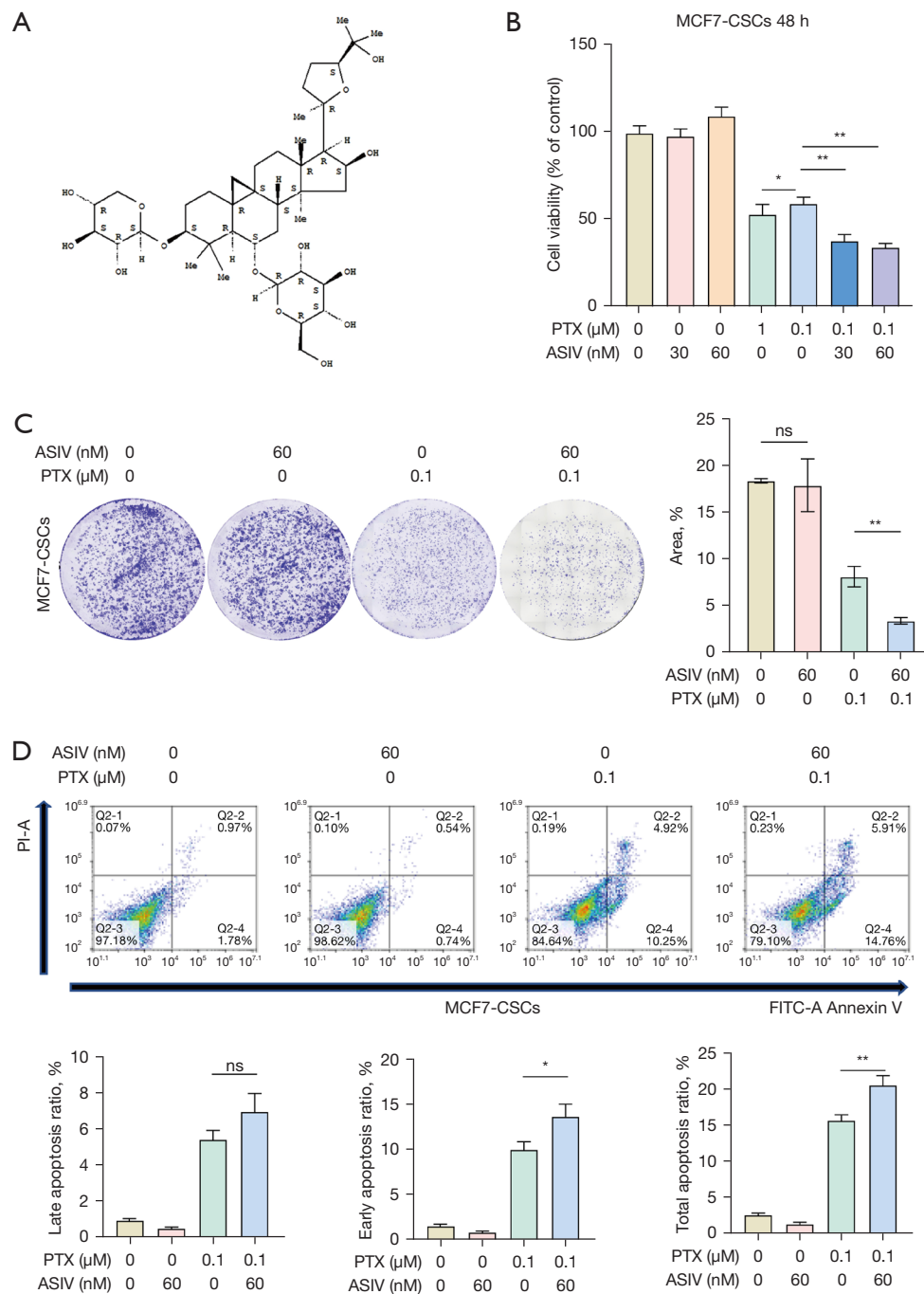


**Figure 2** *In vitro* experiments showed that ASIV increased the sensitivity of BCSCs to PTX. (A) The chemical structure of ASIV. (B) MCF7-CSCs were treated with different concentrations of ASIV, PTX, and their mixture for 48 h, and the cell viability of each group was detected using the CCK-8. (C) Clone formation assay was used to detect the proliferation of MCF7-CSCs after 48 h of treatment with different drugs. 4,000 MCF7-CSCs cells homogeneously seeded in 12-well plates, cells were treated with different drugs for 48 h, drugs were removed, and cell culture continued for 12 d. Formaldehyde fixed, crystal violet stained. (D) MCF7-CSCs were treated with different drugs for 48 h, and apoptosis was detected by flow cytometry. Student's *t*-test: \*,  $P < 0.05$ ; \*\*,  $P < 0.01$ ; ns, not statistically significant. PTX, paclitaxel; ASIV, astragaloside IV; CSCs, cancer stem cells; PI, propidium iodide; FITC, fluorescein isothiocyanate; BCSCs, breast cancer stem cells; CCK-8, Cell Counting Kit-8.



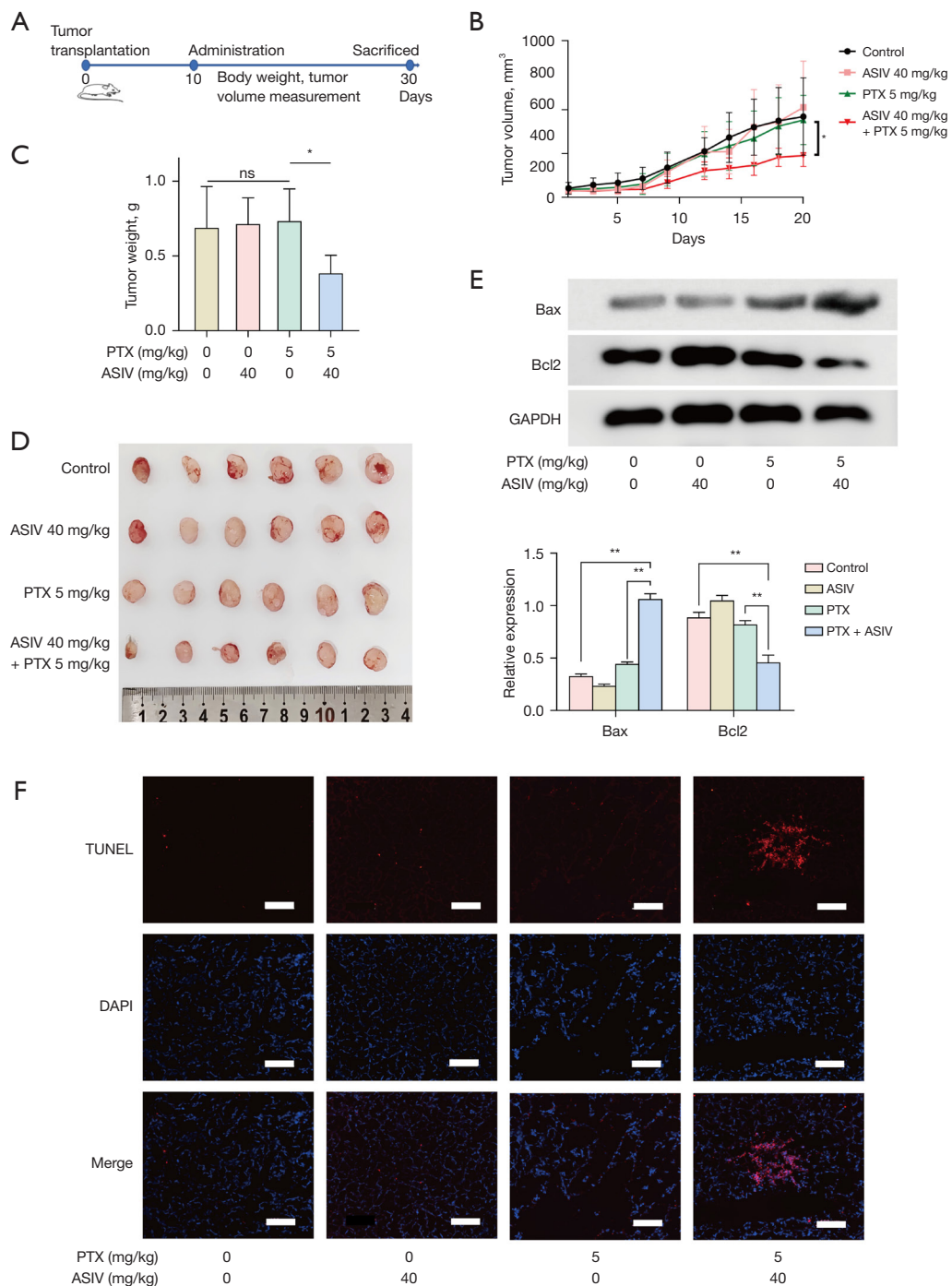


**Figure 3** *In vivo*, ASIV increased the sensitivity of BCSCs to PTX. (A) An orthotopic injection of MCF7-CSCs was used to establish the mouse breast cancer transplantation model. After 10 days, upon reaching a tumor volume of approximately 100 mm<sup>3</sup>, ASIV and PTX were used, and the mice's tumor size and body weight were recorded. (B) Tumor growth curve of each group of mice. (C) Final tumor weight of mice in each group. (D) Tumor image in each group of mice. (E) Western blotting was used to detect the expression of apoptosis-related proteins Bax/Bcl2 in the tumor tissues. (F) TUNEL staining was used to detect apoptosis in the tumor tissue (scale bar: 100 μm). Student's *t*-test: \*, *P* < 0.05; \*\*, *P* < 0.01; ns, not statistically significant. ASIV, astragaloside IV; PTX, paclitaxel; TUNEL, terminal deoxynucleotidyl transferase dUTP nick end labeling; DAPI, 4',6-diamidino-2-phenylindole; BCSCs, breast cancer stem cells; CSCs, cancer stem cells.

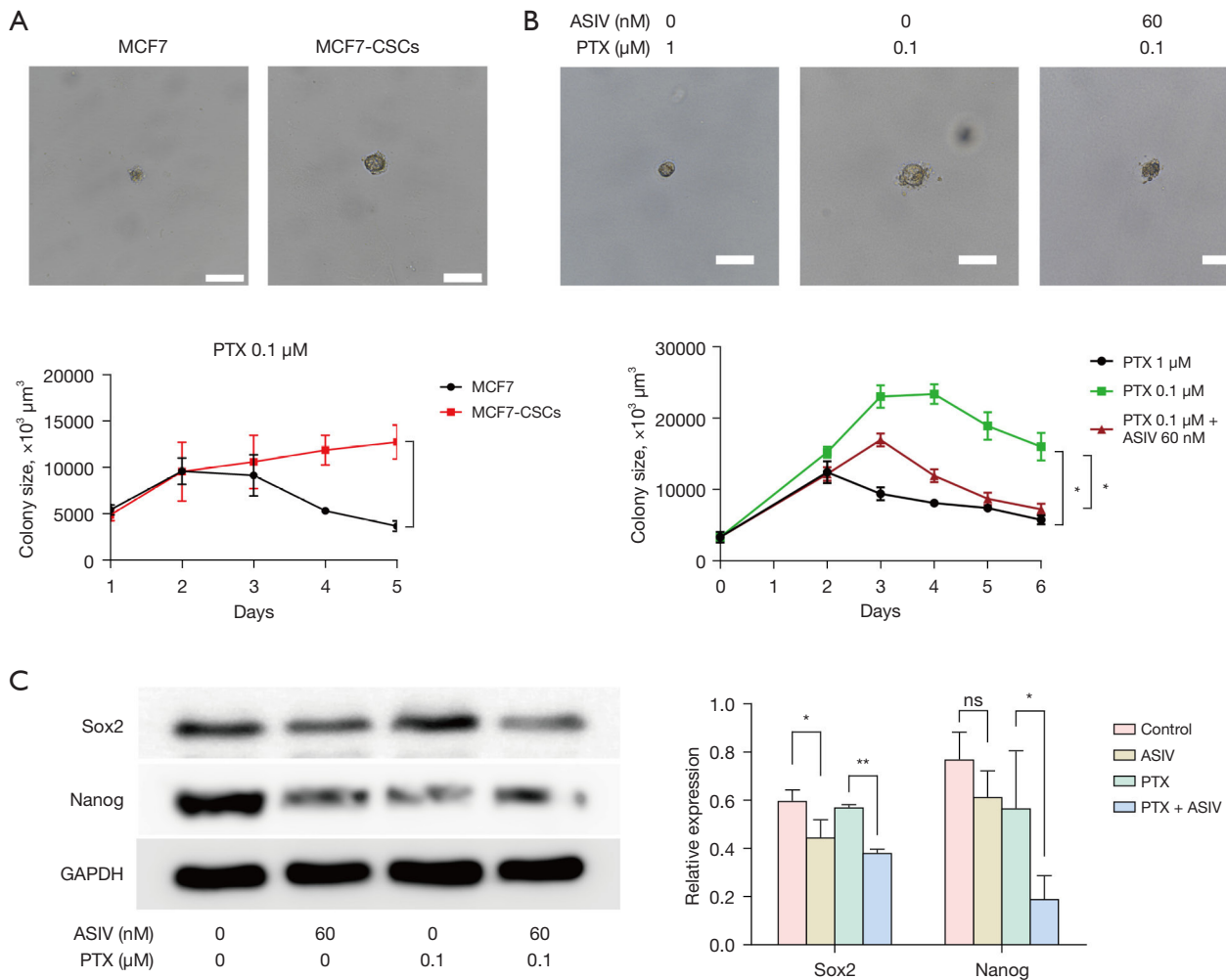


**Figure 4** *In vitro* experiments showed that ASIV combined with PTX can reduce the expression of BCSC markers. (A) 3D tumor spheres assay was used to detect the effect of PTX on MCF7 and MCF7-CSCs (scale bar: 50  $\mu\text{m}$ ). (B) PTX at 1  $\mu\text{M}$  and 0.1  $\mu\text{M}$ , and 0.1  $\mu\text{M}$  PTX + 60 nM ASIV were used for the formation of 3D tumor spheres of MCF7-CSCs to evaluate whether ASIV affected the stemness of MCF7-CSCs (scale bar: 50  $\mu\text{m}$ ). (C) MCF7-CSCs were treated with 0.1  $\mu\text{M}$  PTX, 60 nM ASIV, and the combination of the two drugs for 48 h, and the expression of stem cell markers was detected by western blotting. \*,  $P < 0.05$ ; \*\*,  $P < 0.01$ ; ns, not statistically significant. CSCs, cancer stem cells; ASIV, astragaloside IV; PTX, paclitaxel; BCSC, breast cancer stem cell; 3D, 3-dimensional.

cell sphere formation under PTX. The stronger stemness of MCF7-CSCs meant that the volume of MCF7-CSCs cell spheres was larger (Figure 4A, Figure S4A). Treatment with the combination of ASIV and PTX significantly reduced the volume of the cell sphere compared with that of PTX alone, indicating that the combination of ASIV and PTX reduced the stemness of MCF7-CSCs (Figure 4B, Figure S4B). The results of WB also confirmed the above: ASIV reduced the levels of the stem cell marker proteins Sox2 and Nanog, which represent cell stemness ability and self-renewal

ability. Sox2 and Nanog expression in the cells treated with PTX and ASIV was lower than that in the cells treated with PTX alone (Figure 4C). In addition, consistent results were also found in tumor tissues. WB, immunofluorescence, and IHC were used to detect the expression of stemness-related markers Sox2 and Nanog in tumor tissues. The results showed that ASIV could reduce the protein expression of Sox2 and Nanog in tumor tissues. The use of ASIV in combination with PTX also decreased the protein expression of Sox2 and Nanog in tumor tissue (Figure 5A-5C). Although

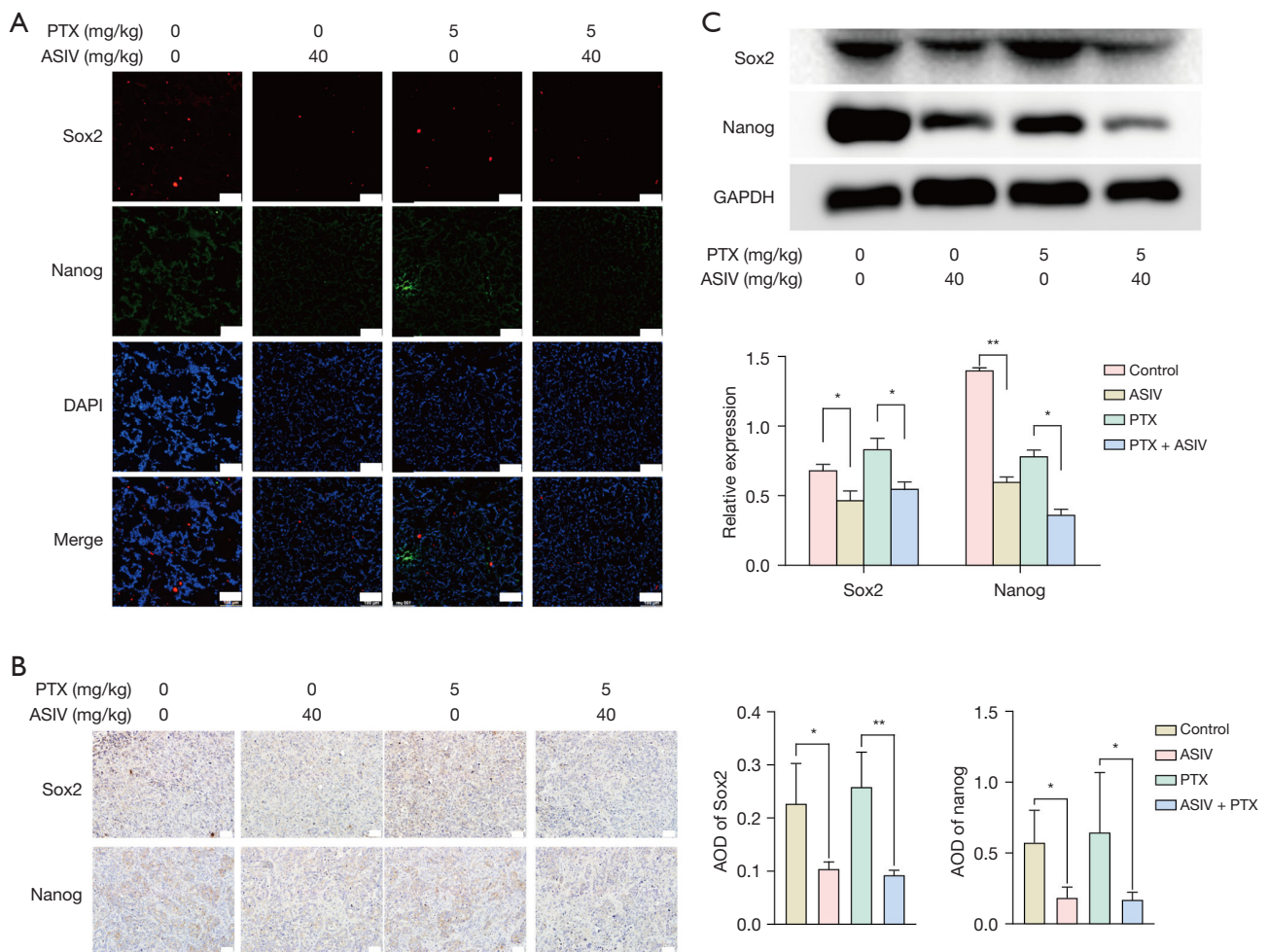


**Figure 5** *In vivo* experiments showed that ASIV combined with PTX decreased the expression of breast cancer stem cell markers. (A) Immunofluorescence detection of stem cell markers in the tumor tissue (scale bar: 100  $\mu$ m). (B) Expression of stem cell markers in the tumor tissues was detected by immunohistochemistry (scale bar: 50  $\mu$ m). (C) Western blotting was used to detect the expression of stem cell markers in the tumor tissues as described above. Student's *t*-test: \*,  $P < 0.05$ ; \*\*,  $P < 0.01$ . PTX, paclitaxel; ASIV, astragaloside IV; DAPI, 4',6-diamidino-2-phenylindole; AOD, average optical density.

ASIV alone did not affect the proliferation of CSCs, ASIV seemed to increase the killing effect of PTX on breast cancer cells by reducing the stemness of CSC.

### Discussion

In this study, by inducing CSCs *in vitro* and transplanted tumor *in vivo*, we found that ASIV combined with PTX, a breast cancer chemotherapy drug, synergistically inhibited the proliferation of CSCs and induced cell apoptosis; this inhibitory effect was achieved by reducing the stemness and self-renewal ability of CSCs.

Chemotherapy is one of the main treatment options for cancer, and resistance to chemotherapy is a major problem facing current cancer research (41,42). Multidrug resistance in cancer cells during chemotherapy can be linked to a range of mechanisms, encompassing enhanced drug efflux, genetic factors such as gene mutations, amplifications, and epigenetic alterations, growth factors, heightened DNA repair capacity, and an elevated metabolism of xenobiotics. Each of these mechanisms results in a diminished therapeutic effectiveness of administered drugs, thereby posing substantial challenges in the anticancer treatment (43). CSCs are a highly tumorigenic subpopulation of tumor cells with

self-renewal ability. Their presence is an important factor affecting the occurrence and development of cancer (12). CSCs possess several self-defense mechanisms to avoid be killed by chemotherapy drugs and show strong resistance to conventional chemotherapy; hence, they are speculated to be a key player in cancer recurrence after chemotherapy (13,44). Chemotherapy is an important treatment for early and advanced breast cancer (9), and BCSCs play an important role in resistance to chemotherapy treatment; thus, targeting or depleting BCSCs can potentially sensitize cancer cells to available drugs (44). A growing number of studies have begun to emphasize the role of bioactive compounds or natural products in plants in cancer chemoprevention (45-48). AM is an important herb that is widely used in the treatment of various cancers (49).

ASIV, one of the major compounds isolated from AM, has anti-tumor effects by inhibiting cell proliferation, invasion, and metastasis of various cancers (50). Our previous experiments have confirmed that ASIV can enhance the chemotherapeutic effect of PTX on breast cancer (37). This study explored the effect of ASIV combined with PTX on BCSCs and further explained the phenomenon of PTX resistance in breast cancer. In recent years, the combination of medicinal plants and cancer chemotherapy has attracted much attention, and it has been found that thymoquinone (TQ) and ginsenoside panaxatriol (GPT) can increase the chemotherapy effect of PTX on breast cancer by inhibiting the stemness of CSC (51,52). The results of this study proved for the first time that ASIV could reduce the stemness of BCSC.

In this study, CSCs with enhanced stemness were successfully induced, and PTX was found to reduce cell proliferation by promoting apoptosis of breast cancer cells. When the stemness increased, the pro-apoptotic effect of PTX on breast cancer cells and the inhibitory effect of PTX on breast cancer cell proliferation were weakened. ASIV combined with PTX promoted the apoptosis of MCF7-CSCs and enhanced the proliferation inhibitory effect on MCF7-CSCs. Interestingly, ASIV alone failed to inhibit the proliferation of MCF7-CSCs. To further understand the mechanism by which ASIV increased the sensitivity of MCF7-CSCs to PTX, we found that ASIV reduced the expression of the stemness markers Sox2/Nanog in MCF7-CSCs. In animal experiments, similar results were observed: ASIV alone could not inhibit the growth of MCF7-CSCs-derived tumors but reduced the stemness of the tumor tissue and enhanced the therapeutic effect of PTX on breast cancer.

These results further suggest that the resistance of breast cancer to PTX may be attributed to the existence of CSCs; ASIV weakened the resistance of MCF7-CSCs to PTX by significantly attenuating the hallmarks of breast cancer stemness and improved the efficacy of PTX in breast cancer.

Numerous studies have shown that hypoxia is closely related to the stemness characteristics of cancer cells. Hypoxia-inducible factor 2 $\alpha$  (HIF-2 $\alpha$ ) is a member of the hypoxia-inducible factor family. HIF-2 $\alpha$  can regulate the self-regeneration ability of BCSC, promote the stemness of breast cancer cells, and affect the chemoresistance of breast cancer to PTX (53,54). By regulating CD44, HIF-2 $\alpha$  enhances PI3K/Akt/mTOR signaling to activate CSC in breast cancer (55). Notch signaling activation promotes BCSC identity and epithelial-mesenchymal transition (56). HIF-2 $\alpha$  promotes the transformation of stem cell phenotype and induces chemoresistance in breast cancer cells by activating Wnt and Notch pathways (39). In addition, some researchers have pointed out that JAK/STAT3-regulated fatty acid  $\beta$ -oxidation is also crucial for BCSC self-renewal and chemotherapy resistance (57). A study on the mechanism of ASIV have shown that ASIV may relieve myocardial cell damage after hypoxia by activating JAK2/STAT3-mediated HIF-1 $\alpha$  signaling (58). In addition, ASIV can inhibit the Notch signaling pathway and PI3K/Akt/mTOR signaling pathway (59,60). Therefore, we hypothesized that the effect of ASIV on the stemness of BCSCs might inhibit the stemness of BCSCs by affecting HIF-1 $\alpha$ /HIF-2 $\alpha$  and inhibiting Notch signal, PI3K/Akt/mTOR or JAK/STAT3 signal transduction. ASIV is the main component of AM, which is a commonly used drug in the treatment of TCM and is widely used in clinical practice, so the discussion of the anti-tumor effect of ASIV has certain value in order to further elucidate the role of AM and optimize the ratio of TCM in clinical application.

## Conclusions

We determined the existence of CSCs as one of the reasons for the resistance of breast cancer to PTX; ASIV weakened the resistance of MCF7-CSCs to PTX by significantly attenuating the hallmarks of breast cancer stemness and improved the efficacy of PTX on breast cancer. ASIV, as an active ingredient of natural drugs, generally considered to be non-toxic, safe, and effective. Our study provides an experimental basis for the adjuvant effect of ASIV in breast cancer chemotherapy. However, our work does not explain how ASIV affects the stemness of tumor cells, so we will

further explore the mechanism of this problem.

## Acknowledgments

*Funding:* This work was supported by the National Natural Science Foundation of China (No. 81974571) and Guangdong Basic and Applied Basic Research Foundation (No. 2022A1515110859).

## Footnote

*Reporting Checklist:* The authors have completed the ARRIVE and MDAR reporting checklists. Available at <https://tcr.amegroups.com/article/view/10.21037/tcr-23-1885/rc>

*Data Sharing Statement:* Available at <https://tcr.amegroups.com/article/view/10.21037/tcr-23-1885/dss>

*Peer Review File:* Available at <https://tcr.amegroups.com/article/view/10.21037/tcr-23-1885/prf>

*Conflicts of Interest:* All authors have completed the ICMJE uniform disclosure form (available at <https://tcr.amegroups.com/article/view/10.21037/tcr-23-1885/coif>). S.R.J. reports grant from Varian Medical Systems to study the oropharyngeal microbiome in HNC patients, and consulting fees from Enlace health to consult on radiation oncology payment models for insurance companies. The other authors have no conflicts of interest to declare.

*Ethical Statement:* The authors are accountable for all aspects of the work in ensuring that questions related to the accuracy or integrity of any part of the work are appropriately investigated and resolved. Animal experiments were performed under a project license (No. 2022008) granted by The Institutional Animal Research Ethics Committee of Guangdong Provincial Hospital of Chinese Medicine, in compliance with national guidelines for the care and use of animals.

*Open Access Statement:* This is an Open Access article distributed in accordance with the Creative Commons Attribution-NonCommercial-NoDerivs 4.0 International License (CC BY-NC-ND 4.0), which permits the non-commercial replication and distribution of the article with the strict proviso that no changes or edits are made and the original work is properly cited (including links to both the

formal publication through the relevant DOI and the license). See: <https://creativecommons.org/licenses/by-nc-nd/4.0/>.

## References

1. Sung H, Ferlay J, Siegel RL, et al. Global Cancer Statistics 2020: GLOBOCAN Estimates of Incidence and Mortality Worldwide for 36 Cancers in 185 Countries. *CA Cancer J Clin* 2021;71:209-49.
2. Allemani C, Matsuda T, Di Carlo V, et al. Global surveillance of trends in cancer survival 2000-14 (CONCORD-3): analysis of individual records for 37 513 025 patients diagnosed with one of 18 cancers from 322 population-based registries in 71 countries. *Lancet* 2018;391:1023-75.
3. Comprehensive molecular portraits of human breast tumours. *Nature* 2012;490:61-70.
4. Allison KH, Hammond MEH, Dowsett M, et al. Estrogen and Progesterone Receptor Testing in Breast Cancer: ASCO/CAP Guideline Update. *J Clin Oncol* 2020;38:1346-66.
5. Wolff AC, Hammond MEH, Allison KH, et al. Human Epidermal Growth Factor Receptor 2 Testing in Breast Cancer: American Society of Clinical Oncology/College of American Pathologists Clinical Practice Guideline Focused Update. *Arch Pathol Lab Med* 2018;142:1364-82.
6. Gennari A, André F, Barrios CH, et al. ESMO Clinical Practice Guideline for the diagnosis, staging and treatment of patients with metastatic breast cancer. *Ann Oncol* 2021;32:1475-95.
7. Debien V, De Caluwé A, Wang X, et al. Immunotherapy in breast cancer: an overview of current strategies and perspectives. *NPJ Breast Cancer* 2023;9:7.
8. Ghislain I, Zikos E, Coens C, et al. Health-related quality of life in locally advanced and metastatic breast cancer: methodological and clinical issues in randomised controlled trials. *Lancet Oncol* 2016;17:e294-304.
9. Cardoso F, Paluch-Shimon S, Senkus E, et al. 5th ESO-ESMO international consensus guidelines for advanced breast cancer (ABC 5). *Ann Oncol* 2020;31:1623-49.
10. Zeng X, Liu C, Yao J, et al. Breast cancer stem cells, heterogeneity, targeting therapies and therapeutic implications. *Pharmacol Res* 2021;163:105320.
11. Saha T, Lukong KE. Breast Cancer Stem-Like Cells in Drug Resistance: A Review of Mechanisms and Novel Therapeutic Strategies to Overcome Drug Resistance. *Front Oncol* 2022;12:856974.
12. Shan NL, Shin Y, Yang G, et al. Breast cancer stem cells:

- A review of their characteristics and the agents that affect them. *Mol Carcinog* 2021;60:73-100.
13. Dean M, Fojo T, Bates S. Tumour stem cells and drug resistance. *Nat Rev Cancer* 2005;5:275-84.
  14. Gudena V, Montero AJ, Glück S. Gemcitabine and taxanes in metastatic breast cancer: a systematic review. *Ther Clin Risk Manag* 2008;4:1157-64.
  15. Pazdur R, Kudelka AP, Kavanagh JJ, et al. The taxoids: paclitaxel (Taxol) and docetaxel (Taxotere). *Cancer Treat Rev* 1993;19:351-86.
  16. Perez EA. Paclitaxel in Breast Cancer. *Oncologist* 1998;3:373-89.
  17. Ahmed Khalil A, Rauf A, Alhumaydhi FA, et al. Recent Developments and Anticancer Therapeutics of Paclitaxel: An Update. *Curr Pharm Des* 2022;28:3363-73.
  18. Rivera E, Gomez H. Chemotherapy resistance in metastatic breast cancer: the evolving role of ixabepilone. *Breast Cancer Res* 2010;12 Suppl 2:S2.
  19. Tolba MF, Esmat A, Al-Abd AM, et al. Caffeic acid phenethyl ester synergistically enhances docetaxel and paclitaxel cytotoxicity in prostate cancer cells. *IUBMB Life* 2013;65:716-29.
  20. Toppmeyer D, Seidman AD, Pollak M, et al. Safety and efficacy of the multidrug resistance inhibitor Incel (biricodar; VX-710) in combination with paclitaxel for advanced breast cancer refractory to paclitaxel. *Clin Cancer Res* 2002;8:670-8.
  21. Farghadani R, Naidu R. Curcumin as an Enhancer of Therapeutic Efficiency of Chemotherapy Drugs in Breast Cancer. *Int J Mol Sci* 2022;23:2144.
  22. Cocco S, Leone A, Roca MS, et al. Inhibition of autophagy by chloroquine prevents resistance to PI3K/AKT inhibitors and potentiates their antitumor effect in combination with paclitaxel in triple negative breast cancer models. *J Transl Med* 2022;20:290.
  23. Fu J, Wang Z, Huang L, et al. Review of the botanical characteristics, phytochemistry, and pharmacology of *Astragalus membranaceus* (Huangqi). *Phytother Res* 2014;28:1275-83.
  24. Guo Z, Lou Y, Kong M, et al. A Systematic Review of Phytochemistry, Pharmacology and Pharmacokinetics on *Astragali Radix*: Implications for *Astragali Radix* as a Personalized Medicine. *Int J Mol Sci* 2019;20:1463.
  25. Li L, Hou X, Xu R, et al. Research review on the pharmacological effects of astragaloside IV. *Fundam Clin Pharmacol* 2017;31:17-36.
  26. Ren S, Zhang H, Mu Y, et al. Pharmacological effects of Astragaloside IV: a literature review. *J Tradit Chin Med* 2013;33:413-6.
  27. Su Y, Xu J, Chen S, et al. Astragaloside IV protects against ischemia/reperfusion (I/R)-induced kidney injury based on the Keap1-Nrf2/ARE signaling pathway. *Transl Androl Urol* 2022;11:1177-88.
  28. Hu T, Fei Z, Wei N. Chemosensitive effects of Astragaloside IV in osteosarcoma cells via induction of apoptosis and regulation of caspase-dependent Fas/FasL signaling. *Pharmacol Rep* 2017;69:1159-64.
  29. Jiang K, Lu Q, Li Q, et al. Astragaloside IV inhibits breast cancer cell invasion by suppressing Vav3 mediated Rac1/ MAPK signaling. *Int Immunopharmacol* 2017;42:195-202.
  30. Li L, Li G, Chen M, et al. Astragaloside IV enhances the sensibility of lung adenocarcinoma cells to bevacizumab by inhibiting autophagy. *Drug Dev Res* 2022;83:461-9.
  31. Li Y, Ye Y, Chen H. Astragaloside IV inhibits cell migration and viability of hepatocellular carcinoma cells via suppressing long noncoding RNA ATB. *Biomed Pharmacother* 2018;99:134-41.
  32. Liu F, Ran F, He H, et al. Astragaloside IV Exerts Anti-tumor Effect on Murine Colorectal Cancer by Re-educating Tumor-Associated Macrophage. *Arch Immunol Ther Exp (Warsz)* 2020;68:33.
  33. Zhou L, Li M, Chai Z, et al. Anticancer effects and mechanisms of astragaloside IV (Review). *Oncol Rep* 2023;49:5.
  34. Shen L, Li Y, Hu G, et al. Astragaloside IV suppresses the migration and EMT progression of cervical cancer cells by inhibiting macrophage M2 polarization through TGFβ/Smad2/3 signaling. *Funct Integr Genomics* 2023;23:133.
  35. Min L, Wang H, Qi H. Astragaloside IV inhibits the progression of liver cancer by modulating macrophage polarization through the TLR4/NF-κB/STAT3 signaling pathway. *Am J Transl Res* 2022;14:1551-66.
  36. Li F, Cao K, Wang M, et al. Astragaloside IV exhibits anti-tumor function in gastric cancer via targeting circRNA dihydrolipoamide S-succinyltransferase (circDLST)/miR-489-3p/ eukaryotic translation initiation factor 4A1(EIF4A1) pathway. *Bioengineered* 2022;13:10111-22.
  37. Zheng Y, Dai Y, Liu W, et al. Astragaloside IV enhances taxol chemosensitivity of breast cancer via caveolin-1-targeting oxidant damage. *J Cell Physiol* 2019;234:4277-90.
  38. Xie XP, Laks DR, Sun D, et al. Quiescent human glioblastoma cancer stem cells drive tumor initiation, expansion, and recurrence following chemotherapy. *Dev Cell* 2022;57:32-46.e8.
  39. Yan Y, Liu F, Han L, et al. HIF-2α promotes conversion

- to a stem cell phenotype and induces chemoresistance in breast cancer cells by activating Wnt and Notch pathways. *J Exp Clin Cancer Res* 2018;37:256.
40. Chen J, Cao X, An Q, et al. Inhibition of cancer stem cell like cells by a synthetic retinoid. *Nat Commun* 2018;9:1406.
  41. Holohan C, Van Schaeybroeck S, Longley DB, et al. Cancer drug resistance: an evolving paradigm. *Nat Rev Cancer* 2013;13:714-26.
  42. Guo X, Gao C, Yang DH, et al. Exosomal circular RNAs: A chief culprit in cancer chemotherapy resistance. *Drug Resist Updat* 2023;67:100937.
  43. Bukowski K, Kciuk M, Kontek R. Mechanisms of Multidrug Resistance in Cancer Chemotherapy. *Int J Mol Sci* 2020;21:3233.
  44. Zhao J. Cancer stem cells and chemoresistance: The smartest survives the raid. *Pharmacol Ther* 2016;160:145-58.
  45. George BP, Chandran R, Abrahamse H. Role of Phytochemicals in Cancer Chemoprevention: Insights. *Antioxidants (Basel)* 2021;10:1455.
  46. Gill C, Walsh SE, Morrissey C, et al. Resveratrol sensitizes androgen independent prostate cancer cells to death-receptor mediated apoptosis through multiple mechanisms. *Prostate* 2007;67:1641-53.
  47. Naeem A, Hu P, Yang M, et al. Natural Products as Anticancer Agents: Current Status and Future Perspectives. *Molecules* 2022;27:8367.
  48. Esmeeta A, Adhikary S, Dharshna V, et al. Plant-derived bioactive compounds in colon cancer treatment: An updated review. *Biomed Pharmacother* 2022;153:113384.
  49. Cho WC, Leung KN. In vitro and in vivo anti-tumor effects of *Astragalus membranaceus*. *Cancer Lett* 2007;252:43-54.
  50. Xia D, Li W, Tang C, et al. Astragaloside IV, as a potential anticancer agent. *Front Pharmacol* 2023;14:1065505.
  51. Bashmail HA, Alamoudi AA, Noorwali A, et al. Thymoquinone Enhances Paclitaxel Anti-Breast Cancer Activity via Inhibiting Tumor-Associated Stem Cells Despite Apparent Mathematical Antagonism. *Molecules* 2020;25:426.
  52. Wang P, Song D, Wan D, et al. Ginsenoside panaxatriol reverses TNBC paclitaxel resistance by inhibiting the IRAK1/NF- $\kappa$ B and ERK pathways. *PeerJ* 2020;8:e9281.
  53. Kise K, Kinugasa-Katayama Y, Takakura N. Tumor microenvironment for cancer stem cells. *Adv Drug Deliv Rev* 2016;99:197-205.
  54. Kim RJ, Park JR, Roh KJ, et al. High aldehyde dehydrogenase activity enhances stem cell features in breast cancer cells by activating hypoxia-inducible factor-2 $\alpha$ . *Cancer Lett* 2013;333:18-31.
  55. Choi S, Yu J, Park A, et al. BMP-4 enhances epithelial mesenchymal transition and cancer stem cell properties of breast cancer cells via Notch signaling. *Sci Rep* 2019;9:11724.
  56. Bai J, Chen WB, Zhang XY, et al. HIF-2 $\alpha$  regulates CD44 to promote cancer stem cell activation in triple-negative breast cancer via PI3K/AKT/mTOR signaling. *World J Stem Cells* 2020;12:87-99.
  57. Wang T, Fahrman JF, Lee H, et al. JAK/STAT3-Regulated Fatty Acid  $\beta$ -Oxidation Is Critical for Breast Cancer Stem Cell Self-Renewal and Chemoresistance. *Cell Metab* 2018;27:136-150.e5. Erratum in: *Cell Metab* 2018;27:1357.
  58. Li B, Yu J, Liu P, et al. Astragaloside IV protects cardiomyocytes against hypoxia injury via HIF-1 $\alpha$  and the JAK2/STAT3 pathway. *Ann Transl Med* 2021;9:1435.
  59. Yao J, Fang X, Zhang C, et al. Astragaloside IV attenuates hypoxia induced pulmonary vascular remodeling via the Notch signaling pathway. *Mol Med Rep* 2021;23:89.
  60. Pei C, Wang F, Huang D, et al. Astragaloside IV Protects from PM2.5-Induced Lung Injury by Regulating Autophagy via Inhibition of PI3K/Akt/mTOR Signaling in vivo and in vitro. *J Inflamm Res* 2021;14:4707-21.

**Cite this article as:** Huang P, Li H, Ren L, Xie H, Chen L, Liang Y, Hu Y, Selistre-de-Araujo HS, Boussios S, Jhawar SR, Cui R, Zuo Q, Chen Q. Astragaloside IV enhances the sensitivity of breast cancer stem cells to paclitaxel by inhibiting stemness. *Transl Cancer Res* 2023;12(12):3703-3717. doi: 10.21037/tcr-23-1885